

Vaccinia Virus Vectors Targeting Peptides for MHC Class II Presentation to CD4⁺ T Cells

Samuel J. Hobbs, Jake C. Harbour, Phillip A. Yates, Diana Ortiz, Scott M. Landfear and Jeffrey C. Nolz

ImmunoHorizons 2020, 4 (1) 1-13

doi: <https://doi.org/10.4049/immunohorizons.1900070>

<http://www.immunohorizons.org/content/4/1/1>

This information is current as of January 3, 2020.

References This article **cites 59 articles**, 26 of which you can access for free at:
<http://www.immunohorizons.org/content/4/1/1.full#ref-list-1>

Email Alerts Receive free email-alerts when new articles cite this article. Sign up at:
<http://www.immunohorizons.org/alerts>

Vaccinia Virus Vectors Targeting Peptides for MHC Class II Presentation to CD4⁺ T Cells

Samuel J. Hobbs,* Jake C. Harbour,* Phillip A. Yates,[†] Diana Ortiz,* Scott M. Landfear,* and Jeffrey C. Nolz*^{‡,§}

*Department of Molecular Microbiology and Immunology, Oregon Health & Science University, Portland, OR 97239; [†]Department of Biochemistry and Molecular Biology, Oregon Health & Science University, Portland, OR 97239; [‡]Department of Cell, Developmental and Cancer Biology, Oregon Health & Science University, Portland, OR 97239; and [§]Department of Radiation Medicine, Oregon Health & Science University, Portland, OR 97239

ABSTRACT

CD4⁺ helper T cells play important roles in providing help to B cells, macrophages, and cytotoxic CD8⁺ T cells, but also exhibit direct effector functions against a variety of different pathogens. In contrast to CD8⁺ T cells, CD4⁺ T cells typically exhibit broader specificities and undergo less clonal expansion during many types of viral infections, which often makes the identification of virus-specific CD4⁺ T cells technically challenging. In this study, we have generated recombinant vaccinia virus (VacV) vectors that target I-A^b-restricted peptides for MHC class II (MHC-II) presentation to activate CD4⁺ T cells in mice. Conjugating the lymphocytic choriomeningitis virus immunodominant epitope GP₆₁₋₈₀ to either LAMP1 to facilitate lysosomal targeting or to the MHC-II invariant chain (Ii) significantly increased the activation of Ag-specific CD4⁺ T cells in vivo. Immunization with VacV-Ii-GP₆₁₋₈₀ activated endogenous Ag-specific CD4⁺ T cells that formed memory and rapidly re-expanded following heterologous challenge. Notably, immunization of mice with VacV expressing an MHC-II-restricted peptide from *Leishmania* species (PEPCK₃₃₅₋₃₅₁) conjugated to either LAMP1 or Ii also generated Ag-specific memory CD4⁺ T cells that underwent robust secondary expansion following a visceral leishmaniasis infection, suggesting this approach could be used to generate Ag-specific memory CD4⁺ T cells against a variety of different pathogens. Overall, our data show that VacV vectors targeting peptides for MHC-II presentation is an effective strategy to activate Ag-specific CD4⁺ T cells in vivo and could be used to study Ag-specific effector and memory CD4⁺ T cell responses against a variety of viral, bacterial, or parasitic infections. *ImmunoHorizons*, 2020, 4: 1–13.

INTRODUCTION

CD4⁺ helper T cells play indispensable roles in shaping many aspects of immunity against a wide variety of infections. Following activation, Th CD4⁺ T cells will differentiate into specialized lineages dictated by the expression of individual transcription factors and functionally defined by the cytokines they then produce. These lineages include Th1 (IFN- γ , TNF- α , and IL-2),

Th2 (IL-4, IL-5, IL-13), Th17 (IL-17) or T follicular helper (provide help to B cells), and the “upstream” signaling pathways that control the commitment to specific Th-lineages has been rigorously defined in vitro (1–3). Although the primary function of CD4⁺ T cells is traditionally considered to be to provide “help” to B cells, macrophages, and cytotoxic CD8⁺ T cells, activated Th1 CD4⁺ T cells also exhibit direct effector functions and are important for controlling many types of viral, bacterial, and parasitic infections.

Received for publication September 3, 2019. Accepted for publication December 16, 2019.

Address correspondence and reprint requests to: Jeffrey C. Nolz, Department of Molecular Microbiology and Immunology, Oregon Health & Science University, 3181 SW Sam Jackson Park Road, Portland, OR 97239. E-mail address: nolz@ohsu.edu

ORCID: 0000-0002-4282-8813 (S.J.H.); 0000-0003-2485-3932 (J.C.H.); 0000-0003-2016-9789 (P.A.Y.); 0000-0001-6492-8842 (D.O.); 0000-0002-1643-6664 (S.M.L.).

This work was supported by grants from the National Institutes of Health (R01-AI132404 [to J.C.N.] and T32-AI007472 [to S.J.H.]).

S.J.H., J.C.H., P.A.Y., and J.C.N. designed and performed experiments and analyzed the data. P.A.Y., D.O., and S.M.L. provided reagents and expertise in experimental design and analysis using *Leishmania* infections. S.J.H. and J.C.N. wrote the manuscript.

Abbreviations used in this article: Ii, MHC-II invariant chain; LAMP1, lysosomal-associated membrane protein 1; LCMV, lymphocytic choriomeningitis virus; MHC-I, MHC class I; MHC-II, MHC class II; PEPCK, phosphoenolpyruvate carboxykinase; VacV, vaccinia virus.

This article is distributed under the terms of the [CC BY 4.0 Unported license](https://creativecommons.org/licenses/by/4.0/).

Copyright © 2020 The Authors

<https://doi.org/10.4049/immunohorizons.1900070>

ImmunoHorizons is published by The American Association of Immunologists, Inc.

In fact, several reports implicate Th1-differentiated CD4⁺ T cells as being the critical cell type that orchestrates antiviral immunity (4–6). Th1-committed effector CD4⁺ T cells are also responsible for controlling a number of nonviral intracellular pathogens, particularly those that reside within phagolysosomes, such as *Mycobacterium tuberculosis* and *Leishmania major* (7–9). Thus, a better understanding of the complex functions of Ag-specific CD4⁺ T cells activated following diverse types of infections or immunizations may allow for improved vaccine design and development, especially against those pathogens that can successfully avoid the antimicrobial activity of neutralizing Abs and/or cytotoxic CD8⁺ T cells.

In contrast to CD8⁺ T cells, which often generate robust Ag-specific responses against viral infections, Ag-specific CD4⁺ T cells in mice typically undergo less expansion and are often difficult to identify using standard immunological assays. In many cases, extensive enrichment with peptide MHC class II (MHC-II) complexes are necessary to detect endogenous, Ag-specific CD4⁺ T cells by flow cytometry (10), even at the peak of the expansion phase. For example, CD4⁺ T cells are known to be critical for controlling vaccinia virus (VacV) infections in both humans and mice, and a number of MHC-II-presented peptides from poxviruses have been identified (11–14). However, the frequency of CD4⁺ T cells specific for an individual VacV epitope is rather small, with the largest reported response being against IIL_{7–21}, representing ~0.15% of CD4⁺ T cells found at the peak of the expansion phase (11). In comparison, the immunodominant CD8⁺ T cell response in C57BL/6 mice (H2-K^b-B8R_{20–27}) expands to account for ~10% of the CD8⁺ T cells following a poxvirus infection (15). In addition to the technical challenges of identifying rare, Ag-specific CD4⁺ T cells following infection or immunization, methods of heterologous challenge that are often employed in studies of memory CD8⁺ T cells are far less used to quantify the protective functions, boosting potentials, and Th lineage plasticity of memory CD4⁺ T cells. Furthermore, the development of experimental reagents for generating Ag-specific memory CD4⁺ T cells by viral immunization could result in understanding the quantitative and qualitative features of memory CD4⁺ T cells that are needed to confer protective immunity against important bacterial or parasitic infections such as tuberculosis or leishmaniasis, where attempts to develop durable, effective vaccines have been unsuccessful (16–18).

Because of the potential utility of VacV as a vaccine vector in humans and as a versatile experimental reagent, in this study, we describe the generation of VacV vectors that express known MHC-II-restricted peptides to activate CD4⁺ T cells in mice. Interestingly, we found that VacV expressing only a minimal peptide sequence was not sufficient to activate CD4⁺ T cells in vivo, but rather required incorporating strategies that would target the peptide for more efficient MHC-II presentation. Immunization of mice with VacV expressing MHC-II-targeted peptides resulted in the generation of highly functional effector and memory CD4⁺ T cells that underwent considerable secondary expansion following heterologous challenge. Finally, we demonstrate that VacV expressing an MHC-II-restricted peptide from

Leishmania species generates polyfunctional Ag-specific memory CD4⁺ T cells that undergo robust re-expansion following a visceral *Leishmania donovani* infection. Overall, our findings show that VacV vectors can be used to activate Ag-specific CD4⁺ T cells, but that targeting the peptides for MHC-II presentation is required. These novel viral vectors will be useful not only for studies of Ag-specific CD4⁺ T cell activation and protective functions during poxvirus infections but also as a vaccine strategy to generate Ag-specific, Th1-differentiated memory CD4⁺ T cells against other relevant pathogens, including *M. tuberculosis*, *L. major*, and *Salmonella enterica*.

MATERIALS AND METHODS

Generation of recombinant VacVs expressing MHC-II-restricted peptides

Recombinant VacVs were generated by homologous recombination into the thymidine kinase gene using the pSC11 vector, as described previously (19). To generate pSC11-GP_{61–80}, annealed oligonucleotides (Integrated DNA Technologies) encoding the GP_{61–80} epitope and containing BglII- and NotI-compatible overhangs were cloned into the pSC11 vector. To generate pSC11-LAMP1, annealed oligonucleotides encoding the lysosomal-associated membrane protein 1 (LAMP1) (National Center for Biotechnology Information reference sequence: NM_010684.3) signal sequence (aa 1–29) and the lysosomal targeting sequence (aa 368–406) were cloned into the BglII and NotI sites of the pSC11 vector, respectively. Oligonucleotides were designed to maintain functional BglII and NotI endonuclease target sequences at the 3' end of the LAMP1 signal sequence (BglII) and 5' end of the lysosome targeting sequence (NotI). Next, oligonucleotides encoding the GP_{61–80} or PEPCK_{335–351} epitope with BglII- and NotI-compatible overhangs were cloned into the pSC11-LAMP1 vector. To generate pSC11 expressing the MHC-II invariant chain (pSC11-Ii), the MHC-II invariant chain (Ii) (National Center of Biotechnology Information reference sequence: NM_010545.3; aa 1–215) was amplified from cDNA synthesized from mouse splenocytes and cloned into the pSC11 vector using the SalI and NotI sites. Annealed oligonucleotides encoding either GP_{61–80} or PEPCK_{335–351} with NotI-compatible overhangs were then cloned into pSC11-Ii. To generate recombinant VacV, BSC-40 cells were infected with VacV-Western Reserve (Biodefense and Emerging Infections Resources) and then transfected with the appropriate vector using FuGENE transfection reagent (Promega). The resulting cell lysate was then used to infect 143B *thymidine kinase*-deficient cells in the presence of BrdU. After three rounds of plaque purification in the presence of BrdU, viruses were screened by DNA sequencing, and successfully recombined viruses were expanded using standard procedures (19).

In vitro infections and plaque assays

For in vitro growth curves, confluent monolayers of BSC-40 cells were infected in 12-well plates in a volume of 200 μ l at 37°C for 1 h. Following infection, cells were scraped, transferred to

microcentrifuge tubes, and subjected to three rounds of freeze-thaw before performing standard plaque assays using BSC-40 cells. For plaque assays of infected skin, ear skin was homogenized in RPMI 1640 medium containing 1% FBS and then subjected to three rounds of freeze-thaw before performing plaque assays using standard protocols. Briefly, serial dilutions were inoculated on BSC-40 cells in a 12-well plate that were then covered with 1% SeaKem agarose in Modified Eagle Medium (Life Technologies). Plaques were visualized 72 h later following overnight incubation with Neutral Red dye.

RT-PCR

BSC-40 cells were infected as described in *In vitro infections and plaque assays*, and 90 min postinfection, RNA was purified using the RNeasy Mini Kit (Qiagen) according to manufacturer's instructions. cDNA was synthesized using the SuperScript First-Strand Synthesis System (Thermo Fisher Scientific) according to manufacturer's instructions. The resulting cDNA was then used as a template for PCR, using DNA primers specific for the GP₆₁₋₈₀ epitope, the LAMP signal sequence and lysosomal targeting sequence (amplifies across GP₆₁₋₈₀), the invariant chain, or hypoxanthine guanine phosphoribosyl transferase (*Hprt*) as a positive control.

Mice and infections

C57BL/6N and C57BL/6J mice (6–10 wk of age, female) were purchased from Charles River/National Cancer Institute and The Jackson Laboratory, respectively. SMARTA and P14 TCR-tg mice have been described previously and were maintained by sibling-with-sibling mating (20, 21). For adoptive transfers, cells were isolated from the spleen and transferred i.v. in a volume of 200 μ l of PBS and mice were infected the following day. VacV and VacV expressing GP₃₃₋₄₁ (VacV-GP₃₃₋₄₁) have been described previously and were generated using standard protocols (19, 22). VacV-GP₃₃₋₄₁ was independently sequenced in our laboratory to confirm only expression of the minimal epitope. VacV skin infections were performed by pipetting 10 μ l of PBS containing 5×10^6 PFU onto the ventral ear skin and poking the ear skin 25–30 times with a 16.5-gauge needle. Lymphocytic choriomeningitis virus (LCMV)–Armstrong infections were performed by injecting 2×10^5 PFU i.p. in PBS. ActA-deficient *Listeria monocytogenes* expressing the GP₃₃₋₄₁ and GP₆₁₋₈₀ epitopes from LCMV (23) was grown in tryptic soy broth (Sigma-Aldrich) supplemented with 50 μ g/ml streptomycin (Sigma-Aldrich) at 37°C until OD₆₀₀ = 0.1 (10^8 CFU/ml), and 5×10^6 CFU were injected i.v. *Leishmania* parasites (*L. donovani* BOB) were routinely cultured at 26°C in RPMI medium supplemented with 25 mM HEPES (pH 6.9), 10 mM glutamine, 7.6 mM hemin, 0.1 mM adenosine, 10% (v/v) heat-inactivated FCS, and 25 μ g/ml G418. The initial density was constantly maintained at 2.5×10^5 cell/ml for no more than six passages. Parasites were grown to the stationary phase, and 5×10^6 parasites were washed twice with PBS and injected i.v.

Quantification of parasite burden

For limiting dilution assays to quantify parasite loads in mice, serial 4-fold dilutions of liver and spleen cell lysates were cultivated in

96-well plates in a *Leishmania* culture medium to which 10% FBS and 100 μ M hypoxanthine were added, as described previously (24). Growth in individual wells was monitored after 2 wk by visual inspection.

Flow cytometry and Abs

The following Abs were used in this study: CD4 (RM4-5; BioLegend), CD8 α (53-6.7; BioLegend), Thy1.1 (OX-7; BioLegend), CD44 (1M7; BioLegend), CD69 (H1.2F3; BioLegend), CD103 (2E7; BioLegend), V α 2 (B20.1; BioLegend), IFN- γ (XMG1.2; BioLegend), TNF- α (MP6-XT22; BioLegend), and IL-2 (JES6-5H4; BioLegend). MHC-II tetramers were obtained from the National Institutes of Health Tetramer Core Facility. Tetramer staining was performed for 1 h at 37°C, and a tetramer loaded with a human CLIP peptide was used as a negative staining control. All other staining was performed for 15–30 min at 4°C. Intravascular labeling was performed as described previously (25). Briefly, 3 μ g of anti-V α 2 was injected i.v. in 200 μ l of PBS, and tissues were harvested 3 min later. Data were acquired using an LSRII Flow Cytometer (BD Biosciences) in the Oregon Health & Science University Flow Cytometry Core Facility. Flow cytometry data were analyzed using FlowJo Software (BD Biosciences) Version 9.9.6 or 10.5.3.

CFSE dilution

Naive Thy1.1⁺ SMARTA CD4⁺ T cells or P14 CD8⁺ T cells were isolated from the spleen and washed twice with PBS before labeling with 1 μ M CFSE at 37°C for 15 min. Cells were then washed twice in RPMI 1640 medium supplemented with 10% FBS and transferred into naive Thy1.2⁺ recipients. The following day, mice were infected on the left ear skin with 5×10^6 PFU of the indicated VacV strain, and proliferation was analyzed by CFSE dilution using FlowJo 9.9.6. The percentage divided and expansion index were calculated using the FlowJo proliferation platform as described previously (26). Briefly, the percentage of cells divided was determined by calculating the average number of divisions of responding cells divided by the average number of divisions of all cells to calculate the proportion of cells that underwent division. The expansion index was calculated by calculating the fold-increase of the number of cells.

Leukocyte isolation from skin

Ears from infected mice were removed, and dorsal and ventral sides of the ear pinna were separated and incubated in 1 ml HBSS (Life Technologies) containing CaCl₂ and MgCl₂ supplemented with 125 U/ml collagenase II (Invitrogen) and DNase-I (Sigma-Aldrich) at 37°C for 1 h. Whole tissue suspensions were then generated by forcing the digested skin through a wire mesh screen. Leukocytes were then purified by resuspending the cells in 10 ml of 35% (v/v) Percoll (GE Healthcare) in HBSS in 50-ml conical tubes followed by centrifugation for 10 min at room temperature.

Ex vivo peptide stimulation and intracellular stain

Spleens from mice were harvested and single cell suspensions were generated by gently forcing the spleen through a mesh screen.

RBCs were lysed by resuspending cell pellets in 150 mM NH₄Cl, 10 mM KHCO₃, and 0.1 mM Na-EDTA. Cells were then washed in RPMI 1640 medium containing 5% FBS and incubated at 37°C in the presence of 2 μM of the indicated peptide and brefeldin A (BioLegend) for 5–6 h. Intracellular cytokine staining was performed using the CytoFix/CytoPerm Kit (BD Biosciences) according to the manufacturer's instructions. Briefly, surface Ags were stained as described in *Flow cytometry and Abs*, followed by permeabilization with 100 μl of CytoFix/CytoPerm for 15 min at 4°C. Staining for cytokines was performed in Perm/Wash Buffer for 20 min at 4°C.

Statistical analyses

Statistics were calculated using Prism Software (GraphPad), using the unpaired Student *t* test or ANOVA with Tukey correction for multiple comparisons.

RESULTS

Generation of VacV vectors that target peptides for MHC-II presentation

To determine whether VacV vectors that express MHC-II-restricted peptides would activate CD4⁺ helper T cells of a desired Ag specificity, we generated recombinant VacV that expresses GP_{61–80} from LCMV, which includes the minimal amino acid sequence required for binding to I-A^b, GP_{66–77} (Fig. 1A; see *Materials and Methods*). In addition, we also generated two additional viruses, incorporating strategies that have been reported to increase the efficiency of MHC-II presentation of Ags in vivo. In one strategy, we generated recombinant VacV expressing GP_{61–80} flanked by two protein sequences of LAMP1, where the N-terminal portion of the protein serves as the signal sequence and the C-terminal sequence targets the chimeric protein to lysosomes (27). As an alternative strategy to direct peptides for MHC-II presentation, we also generated VacV where Ii was directly conjugated to the N terminus of GP_{61–80} (28). All viruses (VacV-GP_{61–80}, VacV-LAMP1-GP_{61–80}, VacV-Ii-GP_{61–80}) exhibited similar growth in BSC-40 cells compared with the *thymidine kinase*-VacV control virus (Fig. 1B). To next verify mRNA expression of the recombinant sequences, we infected BSC-40 cells with VacV expressing GP_{61–80}, LAMP1-GP_{61–80}, or Ii-GP_{61–80} and analyzed expression of the cloned inserts using RT-PCR. Amplification of cDNA synthesized from VacV-infected cells using GP_{61–80}-specific primers demonstrated that all three viruses expressed the GP_{61–80} sequence (Fig. 1C). To next confirm expression of the GP_{61–80} chimeric proteins, we also used primers that specifically amplified LAMP1-GP_{61–80} or Ii-GP_{61–80}. Thus, these data demonstrate the successful generation of recombinant VacV expressing GP_{61–80} alone or conjugated to other protein sequences that have been reported to target Ags for MHC-II presentation.

VacVs that target GP_{61–80} for MHC-II presentation activate Ag-specific CD4⁺ T cells in vivo

Because our in vitro analysis demonstrated that all recombinant viruses exhibited similar growth and expressed the correct

variations of the GP_{61–80} peptide sequence, we next tested whether they would be presented by MHC-II to activate CD4⁺ T cells in vivo. We labeled naive Thy1.1⁺ SMARTA TCR-tg CD4⁺ T cells (specific for I-A^b-GP_{66–77} (20)) with CFSE and transferred them into naive B6 mice. The left ear skin was then infected with VacV or each of the VacV strains expressing GP_{61–80}. On day 3 postinfection, all viruses caused similarly high levels of infection in the skin (Fig. 2A). Surprisingly, VacV expressing only the GP_{61–80} peptide did not stimulate any detectable proliferation of naive SMARTA CD4⁺ T cells in the draining lymph node, suggesting the peptide sequence was not being efficiently presented on MHC-II to CD4⁺ T cells (Fig. 2B), whereas VacV expressing GP_{61–80} conjugated to either LAMP1 or Ii caused significant levels of proliferation (Fig. 2B–D). Activation of naive CD4⁺ T cells was site specific, as proliferation was not detected in contralateral non-draining lymph nodes. Notably, VacV-Ii-GP_{61–80} infection consistently caused more expansion of SMARTA CD4⁺ T cells compared with the LAMP1-conjugated sequence (Fig. 2D), which could be due to less MHC-II presentation using this strategy or because it has also been reported that cathepsin D cleaves the GP_{61–80} sequence (between aa 74 and 75) within lysosomes (29). In contrast, VacV expressing only the MHC class I (MHC-I)-restricted peptide GP_{33–41} from LCMV caused proliferation of naive, Ag-specific P14 TCR-tg CD8⁺ T cells (Fig. 2E–G), demonstrating that VacV expression of minimal MHC-I-restricted peptides is sufficient to activate naive CD8⁺ T cells. Therefore, these data show that targeting peptides for MHC-II presentation is necessary to activate Ag-specific CD4⁺ T cells during VacV skin infection.

The previous data demonstrated that VacV expressing GP_{61–80} conjugated to Ii was the more efficient strategy to activate naive CD4⁺ T cells in vivo. Therefore, we next tested whether viral immunization would stimulate a systemic response that resulted in the generation of memory CD4⁺ T cells. We again transferred naive SMARTA CD4⁺ T cells into B6 mice and infected them with VacV-Ii-GP_{61–80} by either i.p. injection or scarification of the skin to determine if route of infection would influence the magnitude of expansion or the formation of memory cells. Both routes of immunization caused significant clonal expansion of SMARTA CD4⁺ T cells compared with a control VacV infection, and at 30 d postinfection, memory cells could be detected in the circulation (Fig. 3A–C). SMARTA CD4⁺ T cells could also be detected in the skin following infection by scarification (but not i.p. infection) after clearance of the viral infection (Fig. 3D), which occurs within 15 d postinfection (30). Most of the SMARTA CD4⁺ T cells in the previously infected skin expressed CD69 (Fig. 3E, 3F), suggesting the development of tissue residency. Interestingly, in contrast to what we and others have shown for tissue-resident CD8⁺ T cells that form following VacV infection (30, 31), the majority of Ag-specific CD4⁺ T cells in the skin did not express CD103 (Fig. 3E, 3F). Despite their lack of CD103 expression, SMARTA CD4⁺ T cells in the skin were protected from i.v. labeling, demonstrating that these T cells reside within the skin parenchyma (Fig. 3G, 3H). Thus, these data demonstrate that immunization with VacV expressing peptides targeted for MHC-II presentation results in the formation of memory CD4⁺ T cells.

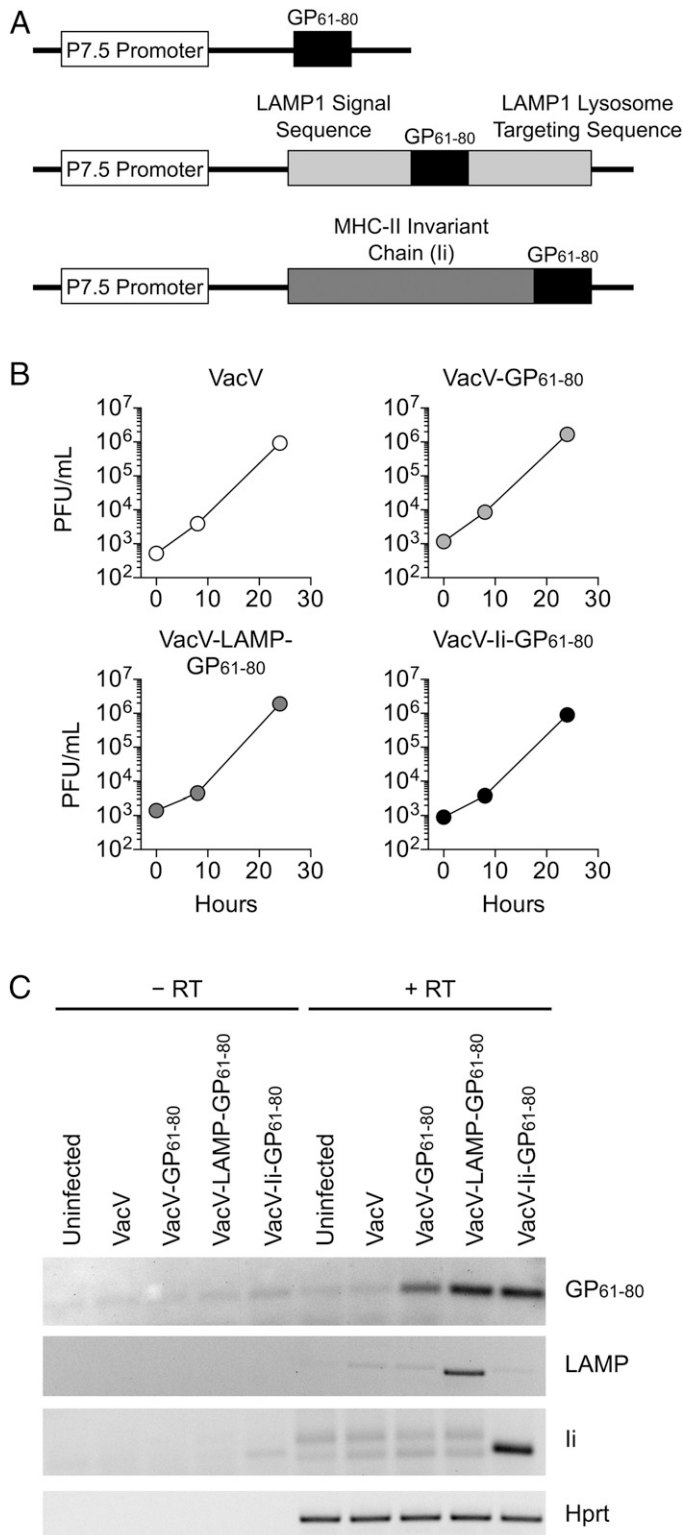


FIGURE 1. Generation of recombinant vaccinia vectors.

(A) Schematic of recombinant pSC11-based VacV vectors expressing GP₆₁₋₈₀. (B) A confluent monolayer of BSC-40 cells were infected with the indicated VacV strain (multiplicity of infection = 0.01) and viral titers were determined at 0, 8, and 24 h postinfection. (C) BSC-40 cells were infected with the indicated strain of VacV (multiplicity of

VacVs that target GP₆₁₋₈₀ for MHC-II presentation activate Ag-specific CD4⁺ T cells within the endogenous repertoire

Using monoclonal TCR-tg SMARTA CD4⁺ T cells as an experimental readout, the previous data demonstrated that peptides required targeting to the MHC-II presentation pathway to stimulate the activation of Ag-specific CD4⁺ T cells in vivo. Therefore, we next determined whether infection with VacV expressing GP₆₁₋₈₀ would also cause the activation and expansion of the rare, Ag-specific CD4⁺ T cells found within the endogenous repertoire. In agreement with our previous data, i.p. immunization with VacV-Ii-GP₆₁₋₈₀, but not VacV-GP₆₁₋₈₀ or VacV-LAMP-GP₆₁₋₈₀, caused expansion of I-A^b-GP₆₆₋₇₇-specific CD4⁺ T cells on day 7 postinfection (Fig. 4A, 4B). Most of the Ag-specific CD4⁺ T cells produced IFN-γ (suggesting Th1-differentiation), and approximately half of the cells exhibited hallmarks of polyfunctionality (e.g., production of TNF-α and IL-2) (Fig. 4C, 4D). Therefore, these data demonstrate that immunization with VacV-Ii-GP₆₁₋₈₀ activates and expands Ag-specific CD4⁺ T cells that exhibit features of Th1 differentiation.

One hallmark of cellular immunological memory is the capacity to undergo more robust re-expansion following heterologous challenge compared with the primary infection. Therefore, we infected mice that had been previously immunized with VacV or VacV-Ii-GP₆₁₋₈₀ with attenuated *L. monocytogenes* expressing the GP₆₁₋₈₀ epitope (23). Upon rechallenge, GP₆₆₋₇₇-specific CD4⁺ T cells underwent robust secondary expansion in mice that had been previously infected with VacV-Ii-GP₆₁₋₈₀, but not VacV (Fig. 4E-G). In fact, the frequency of boosted GP₆₆₋₇₇-specific CD4⁺ T cells in the circulation was ~10 times higher compared with mice receiving control VacV immunization. Overall, these data demonstrate that immunization with VacV-Ii-GP₆₁₋₈₀ generates functional effector and memory CD4⁺ T cells that are able to rapidly expand following secondary challenge.

GP₆₆₋₇₇-specific memory CD4⁺ T cells become reactivated and provide protection following VacV-Ii-GP₆₁₋₈₀ skin infection

Because our data demonstrated that VacV-Ii-GP₆₁₋₈₀ caused the activation of naive Ag-specific CD4⁺ T cells, we next tested whether MHC-II-targeted peptides would reactivate an established memory CD4⁺ T cell population. To test this, we infected naive B6 mice with LCMV, which generates I-A^b-GP₆₆₋₇₇-specific memory CD4⁺ T cells that can be identified in the circulation (Fig. 5A). We then challenged LCMV-immune mice or naive controls on the left ear skin with VacV-Ii-GP₆₁₋₈₀ (Fig. 5B). On day 7 postinfection, GP₆₆₋₇₇-specific memory CD4⁺ T cells in LCMV-immune mice had undergone an ~5-fold re-expansion in the

infection = 0.01), and 90 min postinfection, expression of the GP₆₁₋₈₀ epitope, LAMP sequences, or the invariant chain was analyzed by RT-PCR (+RT). To rule out amplification of genomic viral DNA, PCR was also performed on cDNA synthesis reactions that did not include reverse transcriptase (-RT).

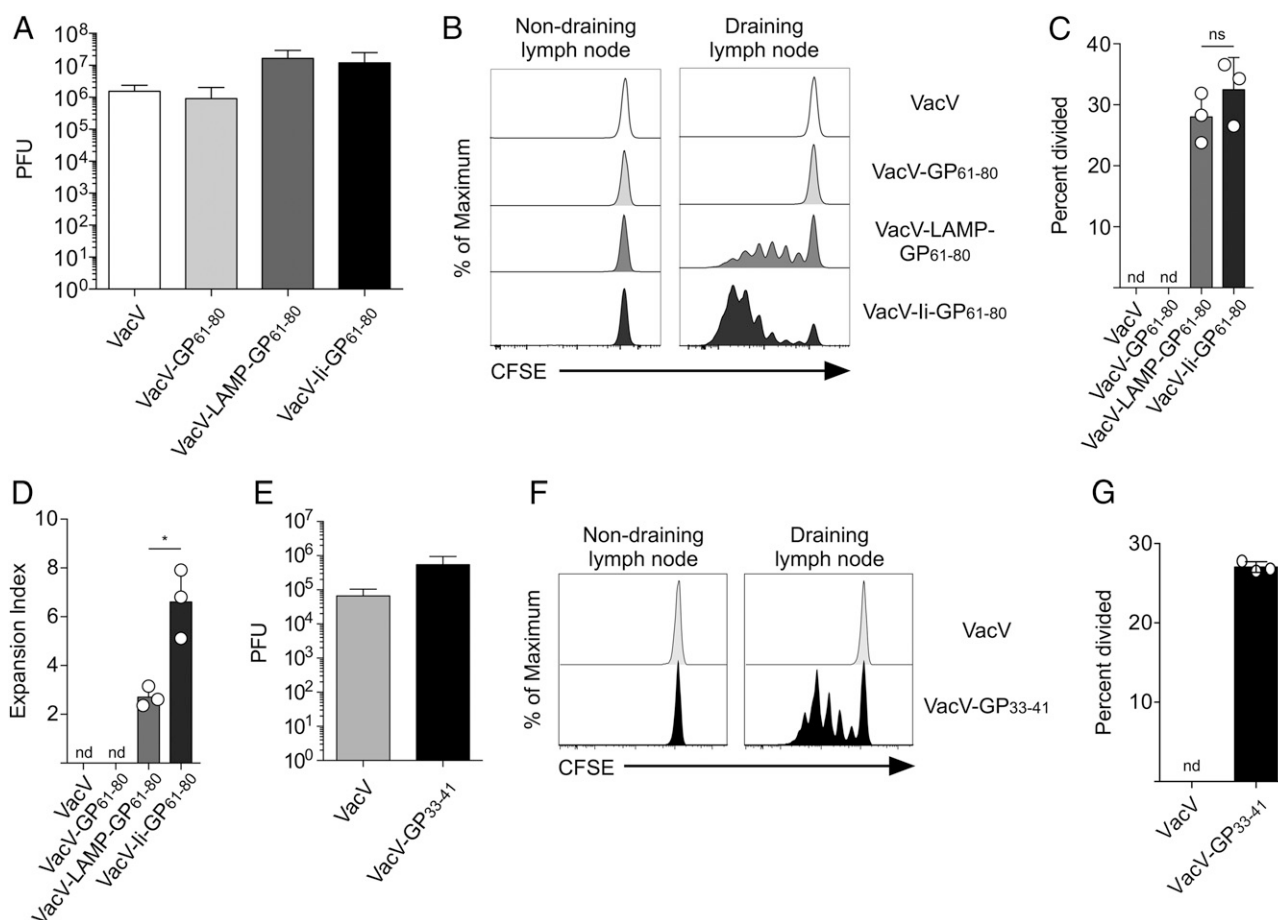


FIGURE 2. VacV vectors designed to enhance MHC-II presentation activate CD4⁺ T cells in vivo.

(A) Naive CFSE-labeled SMARTA CD4⁺ T cells (2×10^6) were transferred into naive B6 mice and were infected on the left ear skin with the indicated strain of VacV, and viral titers in the ear skin were determined 72 h postinfection. (B) CFSE dilution by SMARTA CD4⁺ T cells in the indicated lymph node was measured by flow cytometry 72 h postinfection. (C) Quantification of the percentage of SMARTA CD4⁺ T cells that underwent division in (B). (D) Quantification of the fold expansion of SMARTA CD4⁺ T cells in (B). (E) Naive CFSE-labeled P14 CD8⁺ T cells (2×10^6) were transferred into naive B6 mice that were infected on the left ear skin with the indicated strain of VacV, and viral titers were determined 48 h postinfection. (F) CFSE dilution by P14 CD8⁺ T cells in the indicated lymph node was measured by flow cytometry 48 h postinfection. (G) Quantification of the percentage of P14 CD8⁺ T cells that underwent division in (F). Data are representative of two independent experiments, $n = 3$ per group. Error bars represent SD. * $p < 0.05$. nd, no data.

draining lymph node (compared with contralateral nondraining lymph node) (Fig. 5C, 5D). Notably, VacV-Ii-GP₆₁₋₈₀ viral load in the skin was significantly lower in LCMV-immune mice (Fig. 5E), suggesting that, like memory CD8⁺ T cells (32, 33), memory CD4⁺ T cells are able to provide protection against poxvirus infection. To test whether memory CD4⁺ T cell-mediated protection was Ag-specific, we infected the ear skin of LCMV-immune mice with VacV, VacV-GP₆₁₋₈₀, or VacV-Ii-GP₆₁₋₈₀. LCMV-immune mice were only protected against VacV-Ii-GP₆₁₋₈₀, (Fig. 5F) demonstrating that protection is both Ag-specific and requires the targeting of antigenic peptides to the MHC-II pathway. Thus, these data reveal that I-A^b-GP₆₆₋₇₇-specific memory CD4⁺ T cells generated by LCMV infection become reactivated following VacV-Ii-GP₆₁₋₈₀ skin infection and also provide protective immunity.

Leishmania-specific memory CD4⁺ T cells are generated following immunization with VacV expressing PEPCK₃₃₅₋₃₅₁ targeted for MHC-II presentation

Using the LCMV model Ag GP₆₁₋₈₀, the previous set of experiments provided strong evidence that expression of MHC-II-restricted peptides by VacV required additional targeting strategies to activate CD4⁺ T cells in vivo. Therefore, we next determined whether this strategy would activate CD4⁺ T cells that are specific for a relevant human pathogen, such as intracellular parasites from the genus *Leishmania*. Notably, in contrast to most viral infections that can also be controlled by cytotoxic CD8⁺ T cells, protective immunity against cutaneous and visceral leishmaniasis is largely mediated by IFN- γ -producing Th1-committed CD4⁺ T cells (34, 35). Because an I-A^b-restricted epitope from *Leishmania* has now been identified within the

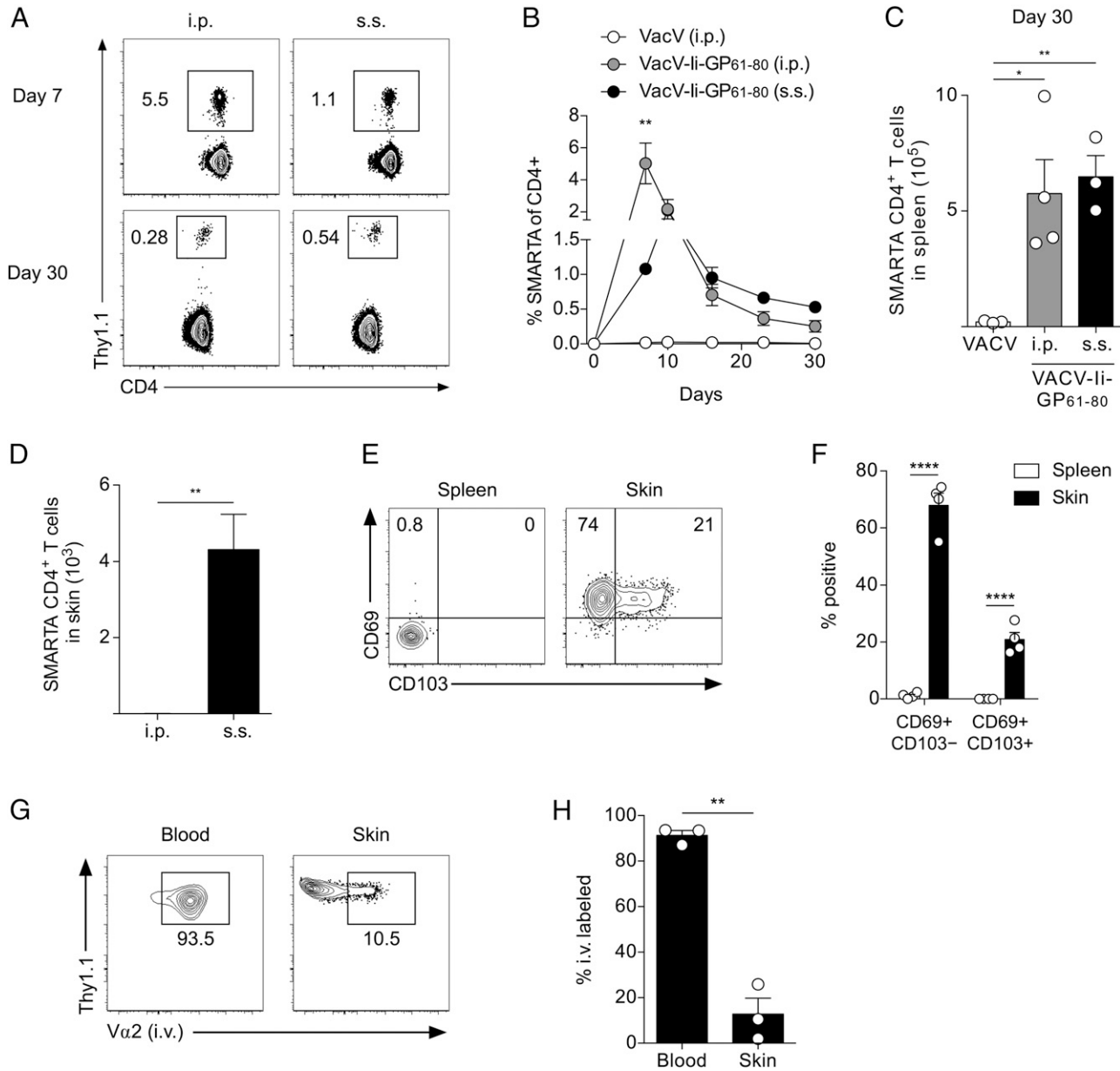


FIGURE 3. Both systemic and localized skin infection with VacV vectors that target GP₆₁₋₈₀ for MHC-II presentation generate memory CD4⁺ T cells.

(A) Naive SMARTA CD4⁺ T cells (2×10^5) were transferred into naive B6 mice that were then infected with VacV or VacV-li-GP₆₁₋₈₀ by either skin scarification (s.s.) or i.p. injection, and SMARTA CD4⁺ T cells were identified in blood on the indicated day postinfection by flow cytometry. (B) Quantification of (A) over time. (C) Quantification of the number of SMARTA CD4⁺ T cells in the spleen 30 d postinfection. (D) The number of SMARTA CD4⁺ T cells in the skin 30 d postinfection was quantified by flow cytometry. (E) Representative flow cytometry plots of CD69 and CD103 expression by SMARTA CD4⁺ T cells from mice infected with VacV-li-GP₆₁₋₈₀ by s.s. (F) Quantification of (E). (G) Representative flow cytometry plots depicting the frequency of i.v.-labeled SMARTA CD4⁺ T cells following VacV-li-GP₆₁₋₈₀ infection by s.s. (H) Quantification of (G). Data are representative of at least two independent experiments, $n = 3-4$ per group. Error bars represent SD. **** $p < 0.0001$, ** $p < 0.01$, * $p < 0.05$.

glycosomal phosphoenolpyruvate carboxykinase (PEPCK) gene, aa 335-351 (36), this presented an opportunity to determine whether Ag-specific memory CD4⁺ T cells could be generated with VacV immunization that would subsequently respond to a *Leishmania* infection. Notably, PEPCK is expressed during both

the promastigote and amastigote stage of the parasite life cycle and its sequence is conserved across *Leishmania* species (36), suggesting it could be a relevant target for rational vaccine design against leishmaniasis. To determine whether memory PEPCK₃₃₅₋₃₅₁-specific CD4⁺ T cells formed following VacV immunization, we

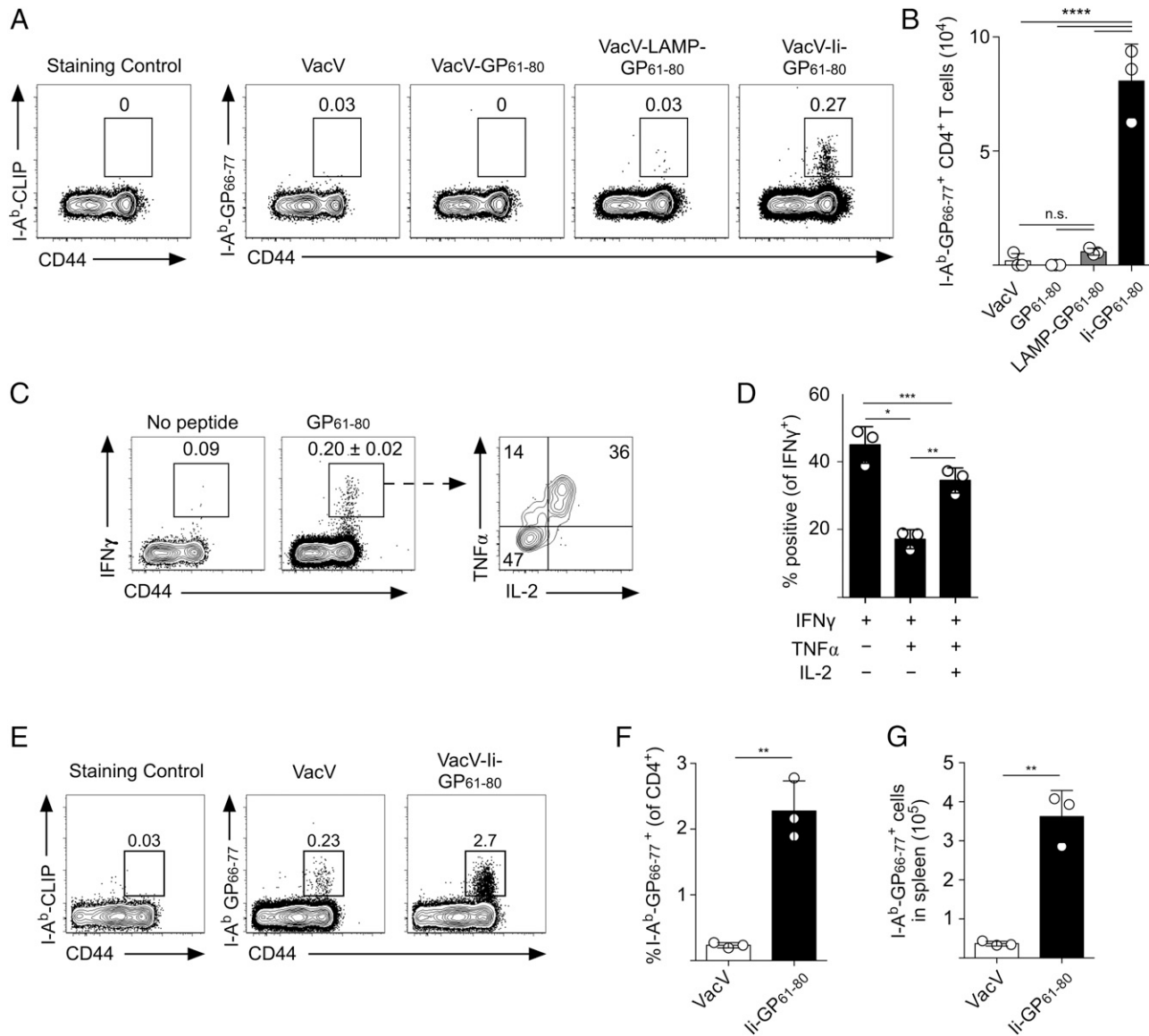


FIGURE 4. VacV vectors that target GP₆₁₋₈₀ for MHC-II presentation generate functional effector and memory CD4⁺ T cells from the endogenous repertoire.

(A) Naive B6 mice were infected with the indicated strain of VacV i.p., and the frequency of I-A^b-GP₆₆₋₇₇-specific CD4⁺ T cells in the spleen on day 7 postinfection was determined by tetramer staining. (B) Quantification of the number of I-A^b-GP₆₆₋₇₇-specific CD4⁺ T cells from (A). (C) Mice were infected with VacV-Ii-GP₆₁₋₈₀ i.p., and cells isolated from the spleen were stimulated with GP₆₁₋₈₀ peptide, and the frequency of IFN- γ , TNF- α , and IL-2-expressing CD4⁺ T cells was determined by flow cytometry. (D) Quantification of (C). (E) Mice were immunized with VacV or VacV-Ii-GP₆₁₋₈₀ as in (A). At 30 d postimmunization, immunized mice were then challenged with *L. monocytogenes* expressing GP₆₁₋₈₀, and I-A^b-GP₆₁₋₈₀-specific CD4⁺ T cells in the blood were identified by tetramer stain 7 d post challenge. (F) Quantification of (E). (G) Quantification of the number of I-A^b-GP₆₁₋₈₀-specific CD4⁺ T cells in the spleen on day 28 post challenge. Data are representative of two independent experiments with $n = 3$ per group. Error bars represent SD. **** $p < 0.0001$, *** $p < 0.001$, ** $p < 0.01$, * $p < 0.05$.

generated VacV-Ii-PEPCK₃₃₅₋₃₅₁ and VacV-LAMP1-PEPCK₃₃₅₋₃₅₁ using the strategies described in Fig. 1A. Naive B6 mice were first immunized with VacV-Ii-PEPCK₃₃₅₋₃₅₁, and at 30 d postinfection, PEPCK₃₃₅₋₃₅₁-specific CD4⁺ T cells were analyzed from the spleen. As predicted, PEPCK₃₃₅₋₃₅₁-specific memory CD4⁺ T cells exhibited a strong Th1-biased lineage commitment and

produced IFN- γ , TNF- α , and IL-2 following stimulation with PEPCK₃₃₅₋₃₅₁ peptide (Fig. 6A-C). Thus, immunization with VacV expressing PEPCK targeted for MHC-II presentation generates Ag-specific, Th1-differentiated memory CD4⁺ T cells.

Because we found that Ag-specific memory CD4⁺ T cells were generated following infection with VacV-Ii-PEPCK₃₃₅₋₃₅₁, we next

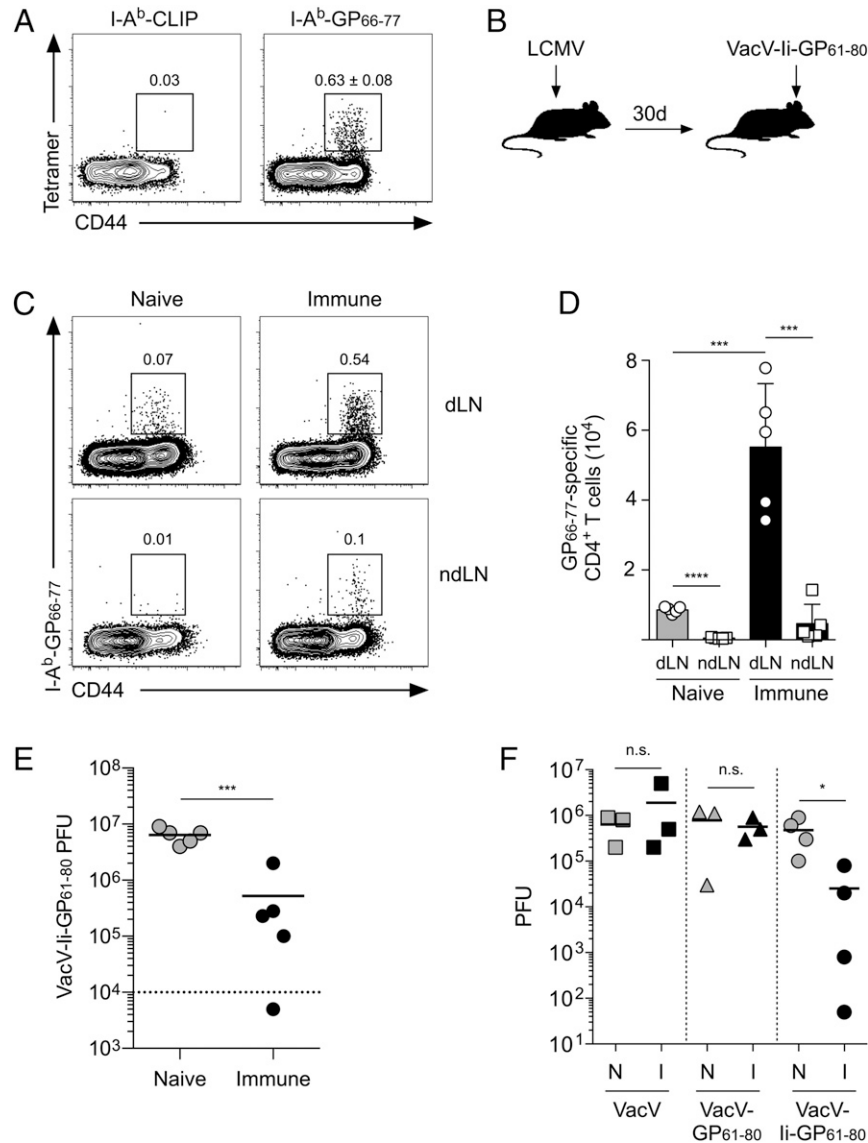


FIGURE 5. Memory CD4⁺ T cells specific for GP₆₆₋₇₇ are reactivated following VacV-Ii-GP₆₁₋₈₀ infection and provide protective immunity.

(A) Naive B6 mice were infected with LCMV, and I-A^b-GP₆₆₋₇₇-specific CD4⁺ T cells were identified in the blood 30 d postinfection by tetramer staining. (B) Experimental design for (C)–(F). (C) On day 7 after VacV challenge, I-A^b-GP₆₆₋₇₇-specific CD4⁺ T cells were identified in the draining (dLN) and nondraining lymph node (ndLN) by tetramer stain. (D) Quantification of (C). (E) Viral titers in the ear skin of naive and LCMV-immune mice 7 d post VacV-Ii-GP₆₁₋₈₀ challenge. (F) Naive and LCMV-immune mice were infected on the left ear skin with the indicated VacV strain, and viral titers were determined 7 d postinfection. Data are representative of two independent experiments with $n = 3-5$ per group. Error bars represent SD. **** $p < 0.0001$, *** $p < 0.001$, * $p < 0.05$. I., LCMV-immune; N., naive.

tested whether this memory CD4⁺ T cell population would undergo re-expansion during a *Leishmania* infection. Interestingly, we found that mice immunized with either the VacV-Ii-PEPCK₃₃₅₋₃₅₁ or VacV-LAMP1-PEPCK₃₃₅₋₃₅₁ caused expansion of endogenous PEPCK₃₃₅₋₃₅₁-specific CD4⁺ T cells in the circulation, demonstrating that, in contrast to LCMV GP₆₁₋₈₀, both strategies efficiently target this peptide for MHC-II presentation in vivo (Fig. 6D). At 25 d postimmunization, we then infected immunized mice with *L. donovani* promastigotes by i.v. injection, which infects the liver and spleen of mice and is used as an experimental model of visceral

leishmaniasis (37). Following challenge with *L. donovani*, PEPCK₃₃₅₋₃₅₁-specific CD4⁺ T cells in mice that had been immunized with the two VacV-PEPCK vectors underwent robust secondary expansion in the circulation, spleen, and liver compared with VacV-immunized controls (Fig. 6D–G). However, despite this robust secondary expansion, parasite burden was not significantly reduced in VacV-PEPCK immunized animals (Fig. 6H, 6I), underscoring the ability of *L. donovani* to evade elimination by the adaptive immune system and highlighting the challenges of developing an effective vaccine against

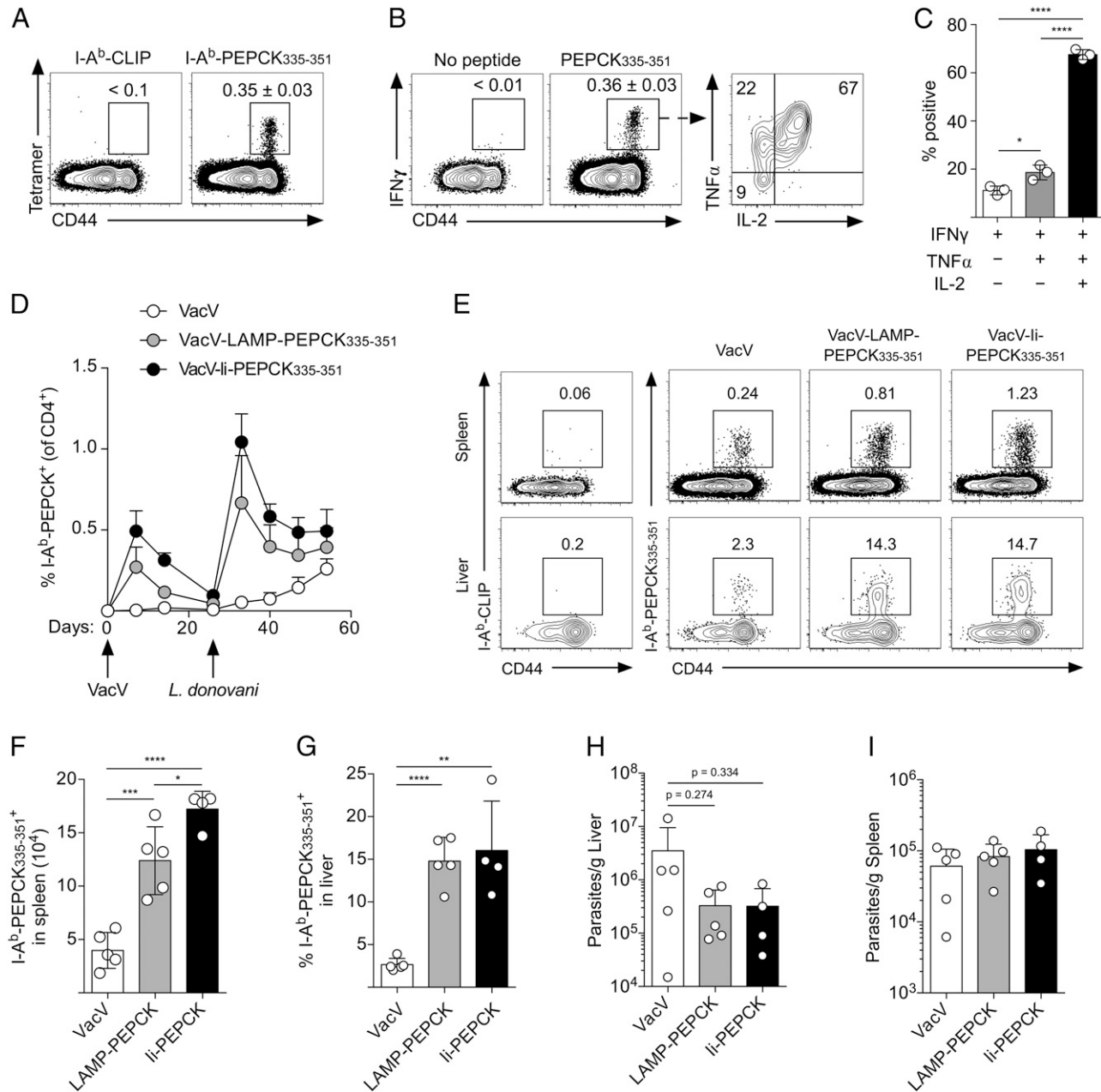


FIGURE 6. Functional *Leishmania*-specific CD4⁺ T cells are generated following infection with VacV vectors that target a *Leishmania* Ag for MHC-II presentation.

(A) Mice were infected with VacV-li-PEPCK₃₃₅₋₃₅₁ i.p., and the frequency of I-A^b-PEPCK₃₃₅₋₃₅₁-specific CD4⁺ T cells in the spleen 30 d postinfection was determined by tetramer staining. (B) Mice were immunized as in (A), and splenocytes were stimulated with PEPCK₃₃₅₋₃₅₁ peptide. The frequency of IFN- γ -, TNF- α -, and IL-2-expressing CD4⁺ T cells was determined by flow cytometry. (C) Quantification of (B). (D) Frequency of I-A^b-PEPCK₃₃₅₋₃₅₁-specific CD4⁺ T cells in the blood following VacV immunization and *L. donovani* challenge. (E) Mice were treated as in (D), and I-A^b-PEPCK₃₃₅₋₃₅₁-specific CD4⁺ T cells were quantified in the liver and spleen on day 25 post *L. donovani* infection by flow cytometry. (F) Quantification of splenic I-A^b-PEPCK-specific CD4⁺ T cells in (E). (G) Quantification of the frequency of I-A^b-PEPCK-specific CD4⁺ T cells in the liver in (E). (H) Parasite burden in the liver. (I) Parasite burden in the spleen. Data are representative of two independent experiments, $n = 3-5$ per group. Error bars represent SD. **** $p < 0.0001$, *** $p < 0.001$, ** $p < 0.01$, * $p < 0.05$.

leishmaniasis. Nevertheless, these data show that VacV vectors targeting a *Leishmania*-specific peptide for MHC-II presentation generates functional memory CD4⁺ T cells that become reactivated during a visceral *Leishmania* infection.

DISCUSSION

It is well established that CD4⁺ T cells play critical roles in protective immunity against a number of intracellular pathogens, but the relevant effector functions and cell types that coordinate memory Th1 CD4⁺ T cell-mediated protective immunity is less clear (38–40). Control of intracellular pathogens, such as *M. tuberculosis* and *Leishmania*, requires Th1-produced IFN- γ and TNF- α to act directly on infected cells. Alternatively, Th1 cytokines can also provide protection by promoting the formation of highly inflammatory tissue microenvironments through the upregulation of chemokines, such as CXCL9 and CXCL10 (41). In contrast to this cytokine-mediated protection, during some viral infections (including poxviruses, CMV, and dengue virus), activated CD4⁺ T cells have been demonstrated to have direct cytotoxic capabilities (42–44). Finally, Ag-specific memory CD4⁺ T cells can also cause more robust maturation of professional APC during viral infection, resulting in stronger priming and expansion of antiviral cytotoxic CD8⁺ T cells (5). Thus, it appears that effector/memory CD4⁺ T cells possess a variety of mechanisms that could contribute to antiviral immunity, but the importance of any individual effector function for controlling diverse types of infections may be highly pathogen- and/or tissue-specific.

How effector and/or memory CD4⁺ T cells recognize intracellular pathogens that result in activation and/or protection remains an active field of research. In the most classic model of MHC-II Ag presentation (45), proteins from the extracellular environment are acquired by phagocytosis or endocytosis that are then delivered into specialized late endosomal/lysosomal Ag-processing compartments that contain a variety of proteases. Following proteolytic cleavage, these processed peptides displace CLIP on recycled MHC-II molecules, which are then transported to the cell surface for presentation to CD4⁺ T cells. However, considerable evidence has accumulated, suggesting that alternative pathways exist that allows cells to directly present cytosolic proteins on MHC-II (46). For example, a recent report found that dendritic cells infected with modified VacV Ankara presented MHC-II-restricted peptides from an endogenous presentation pathway to CD4⁺ T cells, a process that required functional proteasomes and autophagy (47). In agreement with this finding, UV-inactivated ectromelia virus (the causative agent of mousepox) does not activate CD4⁺ T cells in vivo (48), suggesting that a live replicating infectious virus is required for optimal Ag processing and subsequent display of viral Ags on MHC-II. Alternative pathways of viral Ag presentation is not likely a feature of only poxviruses, as CD4⁺ T cell responses to an alternatively presented Ag have been described for several different viruses, including influenza, CMV, and HIV (49–51). Our study suggests that in VacV-infected cells, cytosolic peptides are

not efficiently presented by an alternative endogenous pathway but that fusion to the invariant chain is an effective strategy to target peptides for MHC-II presentation. Finally, it is becoming evident that expression of MHC-II is not restricted to only professional APCs and B cells but can be induced on some nonhematopoietic cells in response to inflammatory cytokines (52–54). Thus, expression of MHC-II on nonhematopoietic cells in combination with nonclassical, endogenous MHC-II Ag presentation could potentially be an important mechanism for effector/memory CD4⁺ T cells to identify and eliminate virally infected cells in nonlymphoid tissues, such as the skin, by either direct cytolytic activity or through the production of antiviral cytokines.

Although memory CD4⁺ T cells clearly play important roles in providing host defense and protective immunity against a variety of pathogens, studies analyzing their formation and differentiation in vivo are far more limited compared with studies of memory CD8⁺ T cells. In particular, the extent of Th lineage commitment and plasticity of Ag-specific memory CD4⁺ T cells following reactivation remains relatively ill-defined. However, recent studies have found that during LCMV or *L. monocytogenes* infections, the majority of activated CD4⁺ T cells exhibit features primarily of the Th1 or T follicular helper lineages and that these commitments appear to be somewhat maintained in the ensuing memory population (55–57). One potential caveat to these studies is that CD4⁺ T cells play little role in protection against these two pathogens, thereby making it difficult to evaluate whether specific T helper lineages of memory CD4⁺ T cells are more protective against reinfection versus another. In fact, it has recently been shown that Ag-specific memory CD4⁺ T cells elicited following immunization become highly pathogenic rather than protective during chronic LCMV infection (58). This contrasts our finding in this study, demonstrating that memory CD4⁺ T cells protect against poxvirus infection, suggesting that the amount of protection provided by memory Th1 CD4⁺ T cells may be highly virus specific (20). Finally, at least in mice, memory CD4⁺ T cell populations seem to be less numerically stable compared with memory CD8⁺ T cells (59), suggesting that frequent “booster” immunization may be necessary to maintain protective levels of memory CD4⁺ T cells (23), but how multiple rounds of Ag stimulation influences T helper lineage commitment, effector functions, or trafficking potentials of memory CD4⁺ T cells remains largely unknown.

In summary, we report the generation of VacV vectors that efficiently target MHC-II-restricted peptides that activate Ag-specific CD4⁺ T cells. Unlike MHC-I-restricted peptides, our findings demonstrate that more complex targeting strategies are required for viral vectors to express Ags that will be presented to CD4⁺ T cells in vivo. Importantly, we show that the Ag-specific memory CD4⁺ T cells generated by viral immunization rapidly respond to heterologous challenge with pathogens expressing the common Ag, demonstrating that this experimental approach may be useful in understanding the extent of protection (or immunopathology) that is provided by memory CD4⁺ T cells against a wide variety of infections. Overall, these viral vectors provide an opportunity to further investigate the activation, lineage commitment,

and effector mechanisms employed by memory CD4⁺ T cells, which could ultimately result in understanding how to improve vaccine strategies against diseases that rely on the protective functions of CD4⁺ T cells.

DISCLOSURES

The authors have no financial conflicts of interest.

ACKNOWLEDGMENTS

We thank Dr. Ann Hill for critical review of the manuscript and also Dr. Jon Yewdell and Dr. James Gibbs for providing the pSC11 plasmid. We would also like to acknowledge the Oregon Health & Science University Flow Cytometry Core Facility.

REFERENCES

- Zhou, L., M. M. Chong, and D. R. Littman. 2009. Plasticity of CD4⁺ T cell lineage differentiation. *Immunity* 30: 646–655.
- O'Shea, J. J., and W. E. Paul. 2010. Mechanisms underlying lineage commitment and plasticity of helper CD4⁺ T cells. *Science* 327: 1098–1102.
- Zhu, J., H. Yamane, and W. E. Paul. 2010. Differentiation of effector CD4⁺ T cell populations (*). *Annu. Rev. Immunol.* 28: 445–489.
- Sant, A. J., and A. McMichael. 2012. Revealing the role of CD4(+) T cells in viral immunity. *J. Exp. Med.* 209: 1391–1395.
- Swain, S. L., K. K. McKinstry, and T. M. Strutt. 2012. Expanding roles for CD4⁺ T cells in immunity to viruses. *Nat. Rev. Immunol.* 12: 136–148.
- Whitmire, J. K. 2011. Induction and function of virus-specific CD4⁺ T cell responses. *Virology* 411: 216–228.
- Tube, N. J., and M. K. Jenkins. 2014. CD4⁺ T Cells: guardians of the phagosome. *Clin. Microbiol. Rev.* 27: 200–213.
- Scott, P., and F. O. Novais. 2016. Cutaneous leishmaniasis: immune responses in protection and pathogenesis. *Nat. Rev. Immunol.* 16: 581–592.
- Scanga, C. A., V. P. Mohan, K. Yu, H. Joseph, K. Tanaka, J. Chan, and J. L. Flynn. 2000. Depletion of CD4(+) T cells causes reactivation of murine persistent tuberculosis despite continued expression of interferon gamma and nitric oxide synthase 2. *J. Exp. Med.* 192: 347–358.
- Moon, J. J., H. H. Chu, J. Hataye, A. J. Pagán, M. Pepper, J. B. McLachlan, T. Zell, and M. K. Jenkins. 2009. Tracking epitope-specific T cells. *Nat. Protoc.* 4: 565–581.
- Moutaftsi, M., H. H. Bui, B. Peters, J. Sidney, S. Salek-Ardakani, C. Oseroff, V. Pasquetto, S. Crotty, M. Croft, E. J. Lefkowitz, et al. 2007. Vaccinia virus-specific CD4⁺ T cell responses target a set of antigens largely distinct from those targeted by CD8⁺ T cell responses. *J. Immunol.* 178: 6814–6820.
- Xu, R., A. J. Johnson, D. Liggitt, and M. J. Bevan. 2004. Cellular and humoral immunity against vaccinia virus infection of mice. *J. Immunol.* 172: 6265–6271.
- Mota, B. E., N. Gallardo-Romero, G. Trindade, M. S. Keckler, K. Kareem, D. Carroll, M. A. Campos, L. Q. Vieira, F. G. da Fonseca, P. C. Ferreira, et al. 2011. Adverse events post smallpox-vaccination: insights from tail scarification infection in mice with Vaccinia virus. *PLoS One* 6: e18924.
- Puissant-Lubrano, B., P. Bossi, F. Gay, J. M. Crance, O. Bonduelle, D. Garin, F. Bricaire, B. Autran, and B. Combadière. 2010. Control of vaccinia virus skin lesions by long-term-maintained IFN-gamma+TNF-alpha+ effector/memory CD4⁺ lymphocytes in humans. *J. Clin. Invest.* 120: 1636–1644.
- Tscharke, D. C., G. Karupiah, J. Zhou, T. Palmore, K. R. Irvine, S. M. Haeryfar, S. Williams, J. Sidney, A. Sette, J. R. Bennink, and J. W. Yewdell. 2005. Identification of poxvirus CD8⁺ T cell determinants to enable rational design and characterization of smallpox vaccines. *J. Exp. Med.* 201: 95–104.
- Andersen, P., and T. M. Doherty. 2005. The success and failure of BCG - implications for a novel tuberculosis vaccine. *Nat. Rev. Microbiol.* 3: 656–662.
- Evans, T. G., L. Schragar, and J. Thole. 2016. Status of vaccine research and development of vaccines for tuberculosis. *Vaccine* 34: 2911–2914.
- Gillespie, P. M., C. M. Beaumier, U. Strych, T. Hayward, P. J. Hotez, and M. E. Bottazzi. 2016. Status of vaccine research and development of vaccines for leishmaniasis. *Vaccine* 34: 2992–2995.
- Wyatt, L. S., P. L. Earl, and B. Moss. 2017. Generation of recombinant Vaccinia viruses. *Curr. Protoc. Protein Sci.* 89: 5.13.1–5.13.18.
- Oxenius, A., M. F. Bachmann, R. M. Zinkernagel, and H. Hengartner. 1998. Virus-specific MHC-class II-restricted TCR-transgenic mice: effects on humoral and cellular immune responses after viral infection. *Eur. J. Immunol.* 28: 390–400.
- Pircher, H., K. Bürki, R. Lang, H. Hengartner, and R. M. Zinkernagel. 1989. Tolerance induction in double specific T-cell receptor transgenic mice varies with antigen. *Nature* 342: 559–561.
- Oldstone, M. B., A. Tishon, M. Eddleston, J. C. de la Torre, T. McKee, and J. L. Whitton. 1993. Vaccination to prevent persistent viral infection. *J. Virol.* 67: 4372–4378.
- Khanolkar, A., M. A. Williams, and J. T. Harty. 2013. Antigen experience shapes phenotype and function of memory Th1 cells. *PLoS One* 8: e65234.
- Wilson, Z. N., C. A. Gilroy, J. M. Boitz, B. Ullman, and P. A. Yates. 2012. Genetic dissection of pyrimidine biosynthesis and salvage in *Leishmania donovani*. *J. Biol. Chem.* 287: 12759–12770.
- Anderson, K. G., K. Mayer-Barber, H. Sung, L. Beura, B. R. James, J. J. Taylor, L. Qunaj, T. S. Griffith, V. Vezys, D. L. Barber, and D. Masopust. 2014. Intravascular staining for discrimination of vascular and tissue leukocytes. *Nat. Protoc.* 9: 209–222.
- Roederer, M. 2011. Interpretation of cellular proliferation data: avoid the panglossian. *Cytometry A* 79: 95–101.
- Wu, T. C., F. G. Guarnieri, K. F. Staveley-O'Carroll, R. P. Viscidi, H. I. Levitsky, L. Hedrick, K. R. Cho, J. T. August, and D. M. Pardoll. 1995. Engineering an intracellular pathway for major histocompatibility complex class II presentation of antigens. *Proc. Natl. Acad. Sci. USA* 92: 11671–11675.
- Holst, P. J., M. R. Sorensen, C. M. Mandrup Jensen, C. Orskov, A. R. Thomsen, and J. P. Christensen. 2008. MHC class II-associated invariant chain linkage of antigen dramatically improves cell-mediated immunity induced by adenovirus vaccines. *J. Immunol.* 180: 3339–3346.
- Rodriguez, F., S. Harkins, J. M. Redwine, J. M. de Pereda, and J. L. Whitton. 2001. CD4(+) T cells induced by a DNA vaccine: immunological consequences of epitope-specific lysosomal targeting. *J. Virol.* 75: 10421–10430.
- Khan, T. N., J. L. Mooster, A. M. Kilgore, J. F. Osborn, and J. C. Nolz. 2016. Local antigen in nonlymphoid tissue promotes resident memory CD8⁺ T cell formation during viral infection. *J. Exp. Med.* 213: 951–966.
- Hobbs, S. J., J. F. Osborn, and J. C. Nolz. 2018. Activation and trafficking of CD8⁺ T cells during viral skin infection: immunological lessons learned from vaccinia virus. *Curr. Opin. Virol.* 28: 12–19.
- Osborn, J. F., S. J. Hobbs, J. L. Mooster, T. N. Khan, A. M. Kilgore, J. C. Harbour, and J. C. Nolz. 2019. Central memory CD8⁺ T cells become CD69⁺ tissue-residents during viral skin infection independent of CD62L-mediated lymph node surveillance. *PLoS Pathog.* 15: e1007633.

33. Osborn, J. F., J. L. Mooster, S. J. Hobbs, M. W. Munks, C. Barry, J. T. Harty, A. B. Hill, and J. C. Nolz. 2017. Enzymatic synthesis of core 2 O-glycans governs the tissue-trafficking potential of memory CD8⁺ T cells. *Sci. Immunol.* 2: eaan6049.
34. Darrach, P. A., D. T. Patel, P. M. De Luca, R. W. Lindsay, D. F. Davey, B. J. Flynn, S. T. Hoff, P. Andersen, S. G. Reed, S. L. Morris, et al. 2007. Multifunctional TH1 cells define a correlate of vaccine-mediated protection against *Leishmania major*. *Nat. Med.* 13: 843–850.
35. Scott, P. 1991. IFN-gamma modulates the early development of Th1 and Th2 responses in a murine model of cutaneous leishmaniasis. *J. Immunol.* 147: 3149–3155.
36. Mou, Z., J. Li, T. Boussoffara, H. Kishi, H. Hamana, P. Ezzati, C. Hu, W. Yi, D. Liu, F. Khadem, et al. 2015. Identification of broadly conserved cross-species protective *Leishmania* antigen and its responding CD4⁺ T cells. *Sci. Transl. Med.* 7: 310ra167.
37. Rodrigues, V., A. Cordeiro-da-Silva, M. Laforge, R. Silvestre, and J. Estaquier. 2016. Regulation of immunity during visceral *Leishmania* infection. *Parasit. Vectors* 9: 118.
38. Soghoian, D. Z., H. Jessen, M. Flanders, K. Sierra-Davidson, S. Cutler, T. Pertel, S. Ransinghe, M. Lindqvist, I. Davis, K. Lane, et al. 2012. HIV-specific cytolytic CD4 T cell responses during acute HIV infection predict disease outcome. *Sci. Transl. Med.* 4: 123ra25.
39. Wilkinson, T. M., C. K. Li, C. S. Chui, A. K. Huang, M. Perkins, J. C. Liebner, R. Lambkin-Williams, A. Gilbert, J. Oxford, B. Nicholas, et al. 2012. Preexisting influenza-specific CD4⁺ T cells correlate with disease protection against influenza challenge in humans. *Nat. Med.* 18: 274–280.
40. Gamadia, L. E., E. B. Remmerswaal, J. F. Weel, F. Bemelman, R. A. van Lier, and I. J. Ten Berge. 2003. Primary immune responses to human CMV: a critical role for IFN-gamma-producing CD4⁺ T cells in protection against CMV disease. *Blood* 101: 2686–2692.
41. Nakanishi, Y., B. Lu, C. Gerard, and A. Iwasaki. 2009. CD8(+) T lymphocyte mobilization to virus-infected tissue requires CD4(+) T-cell help. *Nature* 462: 510–513.
42. Fang, M., N. A. Siciliano, A. R. Hersperger, F. Roscoe, A. Hu, X. Ma, A. R. Shamsdeen, L. C. Eisenlohr, and L. J. Sigal. 2012. Perforin-dependent CD4⁺ T-cell cytotoxicity contributes to control a murine poxvirus infection. *Proc. Natl. Acad. Sci. USA* 109: 9983–9988.
43. Pachnio, A., M. Ciaurritz, J. Begum, N. Lal, J. Zuo, A. Beggs, and P. Moss. 2016. Cytomegalovirus infection leads to development of high frequencies of cytotoxic virus-specific CD4⁺ T cells targeted to vascular endothelium. *PLoS Pathog.* 12: e1005832.
44. Weiskopf, D., D. J. Bangs, J. Sidney, R. V. Kolla, A. D. De Silva, A. M. de Silva, S. Crotty, B. Peters, and A. Sette. 2015. Dengue virus infection elicits highly polarized CX3CR1⁺ cytotoxic CD4⁺ T cells associated with protective immunity. *Proc. Natl. Acad. Sci. USA* 112: E4256–E4263.
45. Roche, P. A., and K. Furuta. 2015. The ins and outs of MHC class II-mediated antigen processing and presentation. *Nat. Rev. Immunol.* 15: 203–216.
46. Veerappan Ganesan, A. P., and L. C. Eisenlohr. 2017. The elucidation of non-classical MHC class II antigen processing through the study of viral antigens. *Curr. Opin. Virol.* 22: 71–76.
47. Thiele, F., S. Tao, Y. Zhang, A. Muschaweckh, T. Zollmann, U. Protzer, R. Abele, and I. Drexler. 2015. Modified vaccinia virus Ankara-infected dendritic cells present CD4⁺ T-cell epitopes by endogenous major histocompatibility complex class II presentation pathways. *J. Virol.* 89: 2698–2709.
48. Forsyth, K. S., B. DeHaven, M. Mendonca, S. Paul, A. Sette, and L. C. Eisenlohr. 2019. Poor antigen processing of Poxvirus particles limits CD4⁺ T cell recognition and impacts immunogenicity of the inactivated vaccine. *J. Immunol.* 202: 1340–1349.
49. Coulon, P. G., C. Richetta, A. Rouers, F. P. Blanchet, A. Urrutia, M. Guerbois, V. Piguat, I. Theodorou, A. Bet, O. Schwartz, et al. 2016. HIV-infected dendritic cells present endogenous MHC class II-restricted antigens to HIV-specific CD4⁺ T cells. *J. Immunol.* 197: 517–532.
50. Miller, M. A., A. P. Ganesan, N. Luckashenak, M. Mendonca, and L. C. Eisenlohr. 2015. Endogenous antigen processing drives the primary CD4⁺ T cell response to influenza. *Nat. Med.* 21: 1216–1222.
51. Hegde, N. R., C. Dunn, D. M. Lewinsohn, M. A. Jarvis, J. A. Nelson, and D. C. Johnson. 2005. Endogenous human cytomegalovirus gB is presented efficiently by MHC class II molecules to CD4⁺ CTL. *J. Exp. Med.* 202: 1109–1119.
52. Santambrogio, L., S. J. Berendam, and V. H. Engelhard. 2019. The antigen processing and presentation machinery in lymphatic endothelial cells. *Front. Immunol.* 10: 1033.
53. Gawkrödger, D. J., M. M. Carr, E. McVittie, K. Guy, and J. A. Hunter. 1987. Keratinocyte expression of MHC class II antigens in allergic sensitization and challenge reactions and in irritant contact dermatitis. *J. Invest. Dermatol.* 88: 11–16.
54. Brown, D. M., S. Lee, M. L. Garcia-Hernandez, and S. L. Swain. 2012. Multifunctional CD4 cells expressing gamma interferon and perforin mediate protection against lethal influenza virus infection. *J. Virol.* 86: 6792–6803.
55. Hale, J. S., B. Youngblood, D. R. Latner, A. U. Mohammed, L. Ye, R. S. Akondy, T. Wu, S. S. Iyer, and R. Ahmed. 2013. Distinct memory CD4⁺ T cells with commitment to T follicular helper- and T helper 1-cell lineages are generated after acute viral infection. *Immunity* 38: 805–817.
56. Marshall, H. D., A. Chandele, Y. W. Jung, H. Meng, A. C. Poholek, I. A. Parish, R. Rutishauser, W. Cui, S. H. Kleinstein, J. Craft, and S. M. Kaech. 2011. Differential expression of Ly6C and T-bet distinguish effector and memory Th1 CD4(+) cell properties during viral infection. *Immunity* 35: 633–646.
57. Pepper, M., A. J. Pagán, B. Z. Igyártó, J. J. Taylor, and M. K. Jenkins. 2011. Opposing signals from the Bcl6 transcription factor and the interleukin-2 receptor generate T helper 1 central and effector memory cells. *Immunity* 35: 583–595.
58. Penaloza-MacMaster, P., D. L. Barber, E. J. Wherry, N. M. Provine, J. E. Teigler, L. Parenteau, S. Blackmore, E. N. Borducchi, R. A. Larocca, K. B. Yates, et al. 2015. Vaccine-elicited CD4 T cells induce immunopathology after chronic LCMV infection. *Science* 347: 278–282.
59. Homann, D., L. Teyton, and M. B. Oldstone. 2001. Differential regulation of antiviral T-cell immunity results in stable CD8⁺ but declining CD4⁺ T-cell memory. *Nat. Med.* 7: 913–919.